© 2019. Published by The Company of Biologists Ltd | Development (2019) 146, dev176784. doi:10.1242/dev.176784

RESEARCH ARTICLE

GPR17 is an essential regulator for the temporal adaptation of sonic hedgehog signalling in neural tube development

Atsuki Yatsuzuka[1], Akiko Hori[1], Minori Kadoya[1], Mami Matsuo-Takasaki[2,*], Toru Kondo[3] and Noriaki Sasai[1,‡]

ABSTRACT

Dorsal-ventral pattern formation of the neural tube is regulated by temporal and spatial activities of extracellular signalling molecules. Sonic hedgehog (Shh) assigns ventral neural subtypes via activation of the Gli transcription factors. Shh activity in the neural progenitor cells changes dynamically during differentiation, but the mechanisms regulating this dynamicity are not fully understood. Here, we show that temporal change of intracellular cAMP levels confers the temporal Shh signal, and the purinergic G-protein-coupled receptor GPR17 plays an essential role in this regulation. GPR17 is highly expressed in the ventral progenitor regions of the neural tube and acts as a negative regulator of the Shh signal in chick embryos. Although the activation of the GPR17-related signal inhibits ventral identity, perturbation of *Gpr17* expression leads to aberrant expansion of ventral neural domains. Notably, perturbation of *Gpr17* expression partially inhibits the negative feedback of Gli activity. Moreover, GPR17 increases cAMP activity, suggesting that it exerts its function by inhibiting the processing of Gli3 protein. GPR17 also negatively regulates Shh signalling in neural cells differentiated from mouse embryonic stem cells, suggesting that GPR17 function is conserved among different organisms. Our results demonstrate that GPR17 is a novel negative regulator of Shh signalling in a wide range of cellular contexts.

KEY WORDS: G-protein-coupled receptor, Chick, Mouse embryonic stem cells, Neural tube, Sonic hedgehog, Temporal adaptation

INTRODUCTION

The neural tube, the embryonic organ of the central nervous system, consists of neural progenitors and post-mitotic neurons arrayed in an orderly manner (Le Dréau and Martí, 2012; Ribes and Briscoe, 2009). During neural tube development, extracellular signalling molecules ('morphogens') produced in the signalling centres of the organ provide positional cues to uncommitted neural progenitor cells, and thereby assign the cellular fates in a concentration-dependent manner (Dessaud et al., 2008). Identifying the molecular mechanism by which cells convert positional information into fate determination is one of the major goals of developmental biology (Dessaud et al., 2008).

Sonic hedgehog (Shh) is a signalling molecule expressed in the floor plate (FP) of the neural tube and its underlying mesodermal tissue, the notochord. Shh plays essential roles in the assignment of ventral identities (Dessaud et al., 2008). At the cellular level, the Shh ligand binds to the 12-domain transmembrane protein patched 1 (Ptch1) at the primary cilia. The binding activates another membrane protein, smoothened (Smo). Smo further activates the transcription factors Gli2 and Gli3, which are transported into the nucleus to induce the expression of their target genes (Dessaud et al., 2008). Gli2 and Gli3 have dual activities; in the absence of Shh, the precursor Gli2 and Gli3 proteins associate with the scaffold protein SuFu to form complexes with cullin 3 and protein kinase A (PKA), and are phosphorylated and proteolytically processed into their repressor forms (Niewiadomski et al., 2014; Tempe et al., 2006; Tuson et al., 2011; Wang and Li, 2006). In response to the Shh ligand, these complexes are dissociated, ubiquitylation is perturbed and Gli2 and Gli3 are converted into their active forms (Niewiadomski et al., 2014; Pan et al., 2006; Wang et al., 2000).

In the spinal cord, Shh forms a ventral-to-dorsal gradient with the highest level in the FP, and is required for the assignment of at least five ventral neural progenitor domains in addition to FP (Dessaud et al., 2008; Ribes and Briscoe, 2009). The ventral domains include p0-p2, pMN and p3, which are arranged in this order from dorsal to ventral, and can be defined by transcription factors expressed in a domain-specific manner. For example, two transcription factors, Olig2 and Nkx2.2, are expressed in the pMN and p3 domains, respectively, and are essential for these identities (Briscoe et al., 1999; Holz et al., 2010; Lu et al., 2000). During the neural tube development, Olig2 responds to Shh and is expressed first; the expression of *Nkx2.2*, which is also regulated by Shh, begins later (Dessaud et al., 2007). The higher concentration of Shh allows the quicker switch from an Olig2- to Nkx2.2-expressing state in the progenitor cells (Dessaud et al., 2010). In this manner, the progenitor cells exposed to a higher Shh concentration form the Nkx2.2-positive p3 domain at a more ventral position than the Olig2/pMN domain. Thus, the Shh gradient is reflected in the dynamic expression of the transcription factors, and various cell types are formed in the spinal cord (Balaskas et al., 2012).

The Gli activity partially reflects the concentration of Shh at the initial step of neural differentiation (Dessaud et al., 2010). After it is initially elevated, however, Gli activity decreases over time (Balaskas et al., 2012; Dessaud et al., 2010). Moreover, the half-life of the signal intensity determines the kinetics of the conversion of the downstream transcription factors that characterise the neural domains. Therefore, the dynamic change of Gli activity, which is termed temporal adaptation, is important for correct pattern formation of the neural tube (Balaskas et al., 2012; Dessaud et al., 2010, 2007; Stamataki et al., 2005).

[1]Developmental Biomedical Science, Graduate School of Biological Sciences, Nara Institute of Science and Technology, 8916-5, Takayama-cho, Ikoma 630-0192, Japan. [2]Department of Regenerative Medicine and Stem Cell Biology, Faculty of Medicine, University of Tsukuba, Tsukuba 305-8575, Japan. [3]Division of Stem Cell Biology, Institute for Genetic Medicine, Hokkaido University, Kita-15, Nishi-7, Kita-Ku, Sapporo 060-0815, Japan.
*Present address: iPS Cell Advanced Characterization and Development Team, RIKEN BioResource Research Center, 3-1-1 Koyadai, Tsukuba, Ibaraki 305-0074, Japan.

‡Author for correspondence (noriakisasai@bs.naist.jp)

N.S., 0000-0003-0360-1138

Received 10 February 2019; Accepted 15 August 2019

Development (2019) 146, dev176784. doi:10.1242/dev.176784

Multiple mechanisms have been proposed to explain this adaptation (Cohen et al., 2015). One model involves upregulation of the *Ptch1* gene. As Ptch1 is a negative regulator of the Shh signal, accumulation of Ptch1 depletes Shh and consequently decreases its intracellular signalling activity (Dessaud et al., 2007). In addition, the expression level of the transcription factor Gli2 decreases over time, and the transduction of the Shh signal is thus reduced as the neural development proceeds (Cohen et al., 2015). Importantly, this adaptation takes place only in the context of the neural differentiation, and not in cultured cells, such as NIH3T3 fibroblast cells (Cohen et al., 2015; Humke et al., 2010; Ribes and Briscoe, 2009), suggesting that some key genes are specifically induced in a developmental context. However, such regulators have yet to be identified.

In parallel with Shh activity, intracellular cyclic AMP (cAMP) level and the activity of the downstream mediator PKA have crucial roles in neural tube pattern formation (Epstein et al., 1996; Tuson et al., 2011). Absence of PKA activity affects the subcellular localisation and processing of Gli proteins at the cellular level, and results in the expansion of the ventral domains of the neural tube (Tuson et al., 2011). Likewise, the activity of adenylyl cyclases 5 and 6 (AC5 and AC6, respectively), which encourage the production of cAMP from adenosine triphosphate (ATP), affects the Gli activity and determination of the ventral cell fate (Moore et al., 2016; Vuolo et al., 2015). Moreover, G-protein-coupled receptors (GPCRs) have been suggested to control the neural tube pattern formation through regulating the intracellular cAMP level (Humke et al., 2010; Pusapati et al., 2018). GPCRs couple with G proteins comprising Gα, Gβ and Gγ subunits. G-proteins are categorised into several subclasses based on the type of the Gα protein; $G\alpha_s$ and $G\alpha_q$ can potentiate the cAMP levels, whereas $G\alpha_i$ decreases this level (Rosenbaum et al., 2009). With respect to the neural tube development and Shh signal, GPR161 has been suggested to interact with $G\alpha_s$ and negatively regulates the ventral neural identities by elevating cAMP levels (Mukhopadhyay et al., 2013). Conversely, GPR175 interacts with $G\alpha_i$ protein and enhances the Shh signal (Singh et al., 2015). Therefore, the GPCR/cAMP/PKA axis is a critical regulatory pathway in the neural tube pattern formation. However, the molecular mechanisms by which cAMP levels and PKA activity are involved in the temporal changes of Gli activity remain to be revealed.

In this study, we found that the PKA activity changes over time in the ventral neural progenitor cells, and thus hypothesised the existence of the regulatory molecule(s) for this change. As cAMP and PKA levels are often regulated by GPCRs, we searched for the GPCRs induced by Shh, and performed a quantitative RT-PCR (RT-qPCR)-based screen in chick neural explants. We consequently identified *Gpr17* as a candidate gene. *Gpr17* is induced by Shh, but negatively regulates the Shh signal. GPR17 also functions as a negative regulator in neural differentiation of mouse embryonic stem (ES) cells. Taken together, our findings demonstrate that GPR17 is a negative regulator of Shh signal in multiple cellular contexts.

RESULTS

Temporal change of PKA activity confers temporal adaptation of the Shh signal

For understanding the mechanisms by which the temporal adaptation (Cohen et al., 2015; Dessaud et al., 2010, 2007) against the Shh signal takes place in the neural progenitor cells, we reasoned that the PKA activity changes over time (Epstein et al., 1996; Tuson et al., 2011; Vuolo et al., 2015). To address this hypothesis, we performed an *ex vivo* analysis using chick intermediate neural explants. We isolated neural progenitor cells from the preneural tube area (Delfino-Machin et al., 2005) of HH stage 9 (Hamburger and Hamilton, 1992) chick embryos and cultured the cells for 24 h. In the explants cultured with the low Shh concentration (Shh^L; see Fig. S1B-H and Materials and Methods), the majority of the cells expressed Olig2 with a small subset of Nkx2.2-positive cells (Fig. 1A,C,E,G). However, in the explants cultured with the PKA inhibitor H-89 together with Shh^L, the Nkx2.2-positive cells dominated the explants (Fig. 1B,D,F,G). As Nkx2.2 is assigned in the more ventral region in the neural tube (Ribes and Briscoe, 2009), this finding suggests that the neural progenitor cells acquired a more ventral identity by blockade of PKA activity. Although it has been shown that the forced downregulation of the PKA activity ventralises the neural identities (Epstein et al., 1996; Hammerschmidt et al., 1996; Vuolo et al., 2015), the explants treated with the sole H-89 did not show any expression of Olig2 or Nkx2.2 (A.Y., N.S., unpublished), suggesting that H-89 does not have the function to mimic the Shh activity at least at this concentration.

Based on this observation, we investigated the relationship between the PKA activity and the temporal change of the intracellular Shh signalling activity, and measured the Gli activity at different time points. We prepared pools of explants transfected with the *GBS-Luc* reporter construct (Sasaki et al., 1999), which harboured the *luciferase* gene driven by the Gli binding sequence (*GBS*). We incubated the explants with Shh^L or Shh^L with H-89 for 6 or 24 h, and measured the Gli activities.

Consistent with the previous reports (Dessaud et al., 2010, 2007), we found upregulated Gli activity 6 h after the starting of the culture (Fig. 1H, lane 1). Importantly, the activity level was comparable with the explants treated with Shh^L and H-89 (Fig. 1H, lane 2), suggesting that the effect of H-89 was not evident at this time point. By contrast, at 24 h, the Gli activity was kept high in the explants with Shh^L and H-89, while the activation was almost undetectable in the explants treated only with Shh^L (Fig. 1H, lanes 3 and 4). This observation suggests that the Gli activity in the neural explants is sensitive to the PKA inhibitor only when cells are at the late (24 h) time point.

It has been suggested that Gli3, a transcription factor that mediates Shh signalling (Litingtung and Chiang, 2000), is destabilised, and the total amount of the full-length and repressor forms of Gli3 is therefore decreased by treatment with Shh (Humke et al., 2010). Therefore, we determined whether the Gli3 levels were affected by the treatment with Shh^L or by the culture period in the explants. We cultured the explants either in the absence or in the presence of Shh^L for different time periods, and examined them by western blots using an anti-Gli3 antibody (Fig. 1I). When cells were treated with Shh^L for 6 h, both the full-length (Gli3FL) and repressor (Gli3R) forms of Gli3 became less abundant, which is consistent with the previous report that Gli3 is destabilised by Shh (Humke et al., 2010) (Fig. 1I, lanes 1 and 2, Fig. 1J). The same trend was found when H-89 was added with Shh^L (Fig. 1I, lanes 2 and 3, Fig. 1J). By contrast, in the explants cultured with Shh^L for 24 h, the processing and the total amount of Gli3 were more similar to those of the untreated explants (Fig. 1I, lanes 4 and 5, Fig. 1J), suggesting that the temporal adaptation corresponds to the dynamic change of the Gli3 processing (Fig. 1H, lane 3). However, this reversion of Gli3 processing by 24 h-Shh^L was perturbed by H-89, suggesting that the temporal Gli3 processing is sensitive to the PKA activity. The Gli3 processing did not significantly change at 6 and 24 h in the untreated explants (Fig. 1I, lanes 3 and 6, Fig. 1J), suggesting that the PKA activity changes only when neural progenitor cells are

Development (2019) 146, dev176784. doi:10.1242/dev.176784

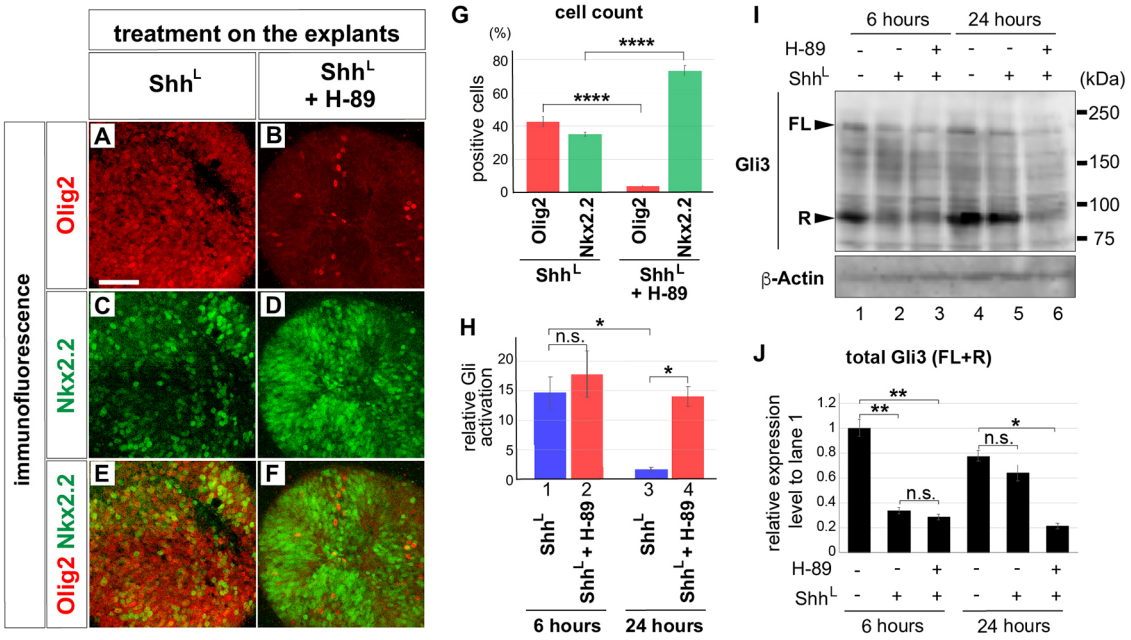

Fig. 1. Temporal change of the intracellular cAMP level confers the temporal adaptation of the neural progenitor cells. (A-F) The intermediate neural explants cultured with Shh^L (A,C,E) or with Shh^L+H-89 (2 µM; B,D,F) for 24 h were analysed by immunofluorescence with anti-Olig2 (A,B,E,F) and -Nkx2.2 (C,D,E,F) antibodies. (G) Quantitative data for A-F. (H) Temporal Gli activities are altered by blocking the PKA activity. Explants electroporated with *GBS-Luc* were incubated with Shh^L or Shh^L+H-89 for 6 or 24 h, and luciferase activities were measured. (I) The processing of the Gli3 protein corresponds to the Gli activities. Western blot analysis was performed in the explants cultured with Shh^L or Shh^L+H-89 for 6 or 24 h, as in H. The full-length (FL) and repressor (R) forms of Gli3 are indicated with arrowheads. (J) The total amounts of Gli3FL and Gli3R in I are quantified. Scale bar: 50 µm.

exposed to Shh. Taken together, the PKA activity changes over time and confers the temporal adaptation of the Shh signal during ventral neural differentiation.

GPR17 is expressed in the ventral region of the neural tube

Based on the observation in Fig. 1, we supposed the existence of the PKA activity-upregulating molecule(s) the expression of which is dependent on Shh. To identify such molecules, we focused on GPCRs, as many GPCRs regulate the activity of PKA and further modify the activities of Gli transcription factors (Moore et al., 2016). With this in mind, we selected genes encoding GPCRs that can bind to $G\alpha_s$ or $G\alpha_q$, and performed a screen that combined RT-qPCR and *in situ* hybridisation (Fig. S2) to isolate the GPCR that responds to Shh. Based on its expression pattern and responsiveness to Shh, we identified the purinergic-like GPCR (a group of GPCRs that take purine as ligand) *Gpr17* as a candidate.

We first investigated the spatio-temporal expression of *Gpr17* in the chick spinal cord, and compared it with that of Olig2 and Nkx2.2 (Fig. 2A-F). *In situ* hybridisation analysis revealed that *Gpr17* was not expressed at HH stage 10, immediately after the neural tube was formed and Olig2 started to be expressed (Fig. 2A,B). At HH stage 14, GPR17 was expressed broadly in the ventral region covering the area where Olig2 and Nkx2.2 are strongly expressed (Fig. 2C,D). At HH stage 24, the *Gpr17* expression formed a dorsal-to-ventral gradient in the progenitor region of the neural tube, with the lowest level at the dorsal region and highest level at Olig2- and Nkx2.2-positive regions, (Fig. 2E,F). In addition, although the expression of *Gpr17* was found in a wide area in the ventral region at the beginning of the neural tube development (Fig. 2C), the floor-plate expression halted as development progressed (Fig. 2E,F).

In the mouse spinal cord, GPR17 expression was evident in the ventral region, including pMN and p3 areas at embryonic day 10.5 (E10.5) when neural tube pattern formation is taking place, as confirmed both by *in situ* hybridisation and immunofluorescence (Fig. S3A,B). This expression pattern was essentially the same as in the developing spinal cord of chicks.

To investigate the relationship between Shh and *Gpr17* expression, we cultured the intermediate neural explants in the presence of Shh^L or Shh^H (see Fig. S1 and Materials and Methods). Expression levels of *Gpr17* were measured by RT-qPCR, every 12 h up to 48 h (Fig. 2G). At 12 h, *Gpr17* expression was higher in explants treated with Shh^L or Shh^H than in untreated explants (Fig. 2G), and this trend continued at 24 and 36 h. By contrast, at 48 h, expression was downregulated in explants treated with Shh^H, but remained high in explants treated with Shh^L. This finding is consistent with the *in vivo* expression pattern of abolished expression in the floor plate (Fig. 2E,F).

Next, we explored the upstream transcription factors that induce *Gpr17* expression. As *Gpr17* requires *Olig1* for its expression (Chen et al., 2009) and is one of the target genes of Olig2 during oligodendrocyte development (Ou et al., 2016), we assessed whether the overexpression of an Olig-type transcription factor could induce the *Gpr17* transcript. To address this, we prepared intermediate neural explants that were electroporated with the *Olig2* expression plasmid, and determined the *Gpr17* expression level by RT-qPCR. *Gpr17* expression was elevated at 24 h, suggesting that Olig2 alone is sufficient to induce it (Fig. 2H, lanes 1 and 2). By contrast, FoxA2, which characterises the floor plate, downregulated *Gpr17* (Fig. 2E, lanes 1 and 3), which was consistent with the observation that the *Gpr17* expression was lower in the floor-plate region. Znf488 (also known as Zfp488), which is expressed in the same regions as *Olig2* (Rehimi et al., 2016; Wang et al., 2006), did not have a significant effect on GPR17 expression (Fig. 2H, lanes 1 and 4). These data supported the idea that *Gpr17* expression is targeted by Olig2 (Ou et al., 2016), and becomes exclusive to the floor plate as development progresses.

Development (2019) 146, dev176784. doi:10.1242/dev.176784

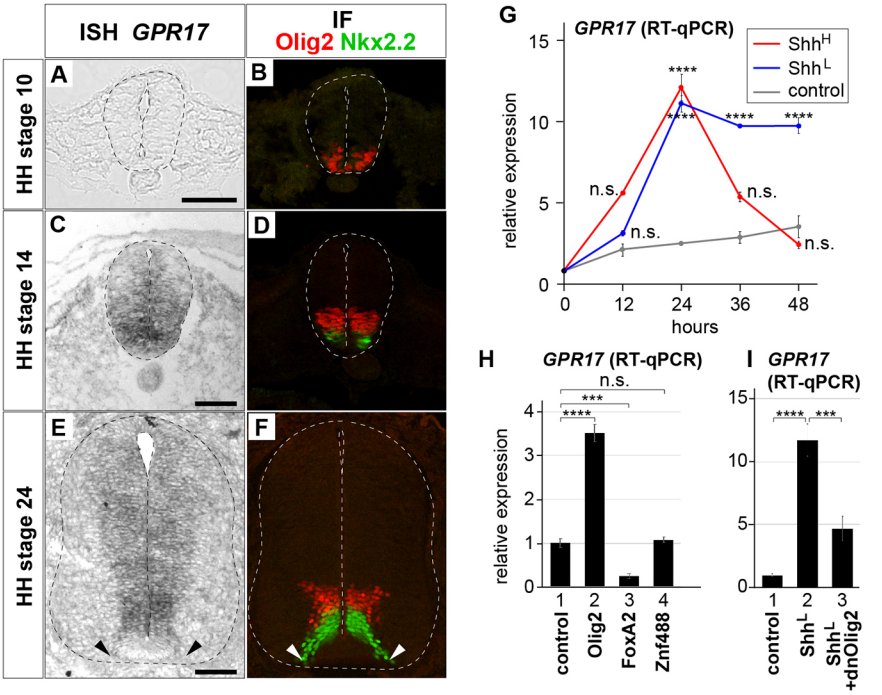

Fig. 2. GPR17 is strongly expressed in ventral progenitor regions of the neural tube. (A-F) Expression of *Gpr17*, Olig2 and Nkx2.2. *In situ* hybridisation analysis of *Gpr17* on a section of trunk neural tube was performed at HH stages 10 (A), 14 (C) and 24 (E), and the expression pattern was compared with those of Olig2 (red) and Nkx2.2 (green), as determined by immunofluorescence (IF) at equivalent stages (B,D,F). The ventral ends of the *Gpr17* (E) and Nkx2.2 (F) expression domains are indicated by arrowheads. Scale bars: 100 µm. (G) The *Gpr17* expression profile was analysed by RT-qPCR in the neural explants cultured in the absence or in the presence of Shh^{L} or Shh^{H} for indicated time periods. (H) The *Gpr17* expression is affected by Olig2 and FoxA2, but not by Znf488. Neural explants electroporated with control GFP (column 1), *Olig2* (column 2), *FoxA2* (column 3) or *Znf488* (column 4) were prepared and the expression of *Gpr17* was analysed by qPCR after the 24 h culture. (I) *Gpr17* expression depends on Olig2. Neural explants electroporated with control GFP (columns 1 and 2) or *dn-Olig2* (column 2) were cultured in the absence (column 1) or in the presence (columns 2 and 3) of Shh^{L} for 24 h, and *Gpr17* expression was analysed by RT-qPCR.

We further investigated the requirement of Olig2 for the expression of *Gpr17*. We prepared the neural explants electroporated with the construct encoding the dominant-negative version of Olig2 (Zhou and Anderson, 2002), and cultured with Shh^{L} for 24 h (Fig. 2I). As a result, the GPR17 expression was downregulated, suggesting that the GPR17 expression requires Olig2 (Fig. 2I).

The collective results suggested that GPR17 expression is mainly regulated by Shh signal and its downstream transcription factor Olig2. This intriguing regulation of *Gpr17* expression prompted us to further investigate its role in neural tube development.

GPR17 is a negative regulator of the Shh signalling pathway

We sought to characterise the molecular role of GPR17 in the Shh signalling pathway, and first analysed the subcellular localisation of GPR17. As Shh signal is mediated the membrane proteins localised to the cilia (Sasai and Briscoe, 2012), we particularly focused on the correlation with the cilia. However, in NIH3T3 cells, GPR17 was not accumulated at the cilia in the normal culture condition (Fig. S4A-C). This localisation did not change upon treatment with Shh (Fig. S4C). Moreover, in the mouse neural tube, GPR17 was not localised to the cilia of the apical surface. (Fig. S3C-G). Therefore the subcellular localisation of GPR17 does not have any correlation with the cilia.

Next, we attempted to examine the effect of GPR17 in the Shh intracellular signalling pathway. For this purpose, we prepared control or *Gpr17*-transfected NIH3T3 cells to assay the expression levels of *Ptch1* and *Gli1*, which are primary target genes of the Shh signal (Cohen et al., 2015) (Fig. 3A). The mere transfection of GPR17 did not affect the expression levels of these genes (Fig. 3A). However, when the cells were treated with purmorphamine (Pur), an agonist of Smo, for 24 h, the extent of the upregulation in *Gpr17*-transfected cells was significantly lower than in the control cells (Fig. 3A). Given that Pur targets the Smo protein (Briscoe, 2006), this result suggests that GPR17 perturbs the intracellular Shh signal at the downstream level of Smo.

We next sought to determine whether the amount of Gli3FL and Gli3R was affected by the overexpression of *Gpr17*. We treated the control or *Gpr17*-transfected cells with Pur, and examined them by western blots using the anti-Gli3 antibody (Fig. 3B). Without Pur treatment, the ratio of the full-length over the repressor form of Gli3 was not changed by the transfection of GPR17 (Fig. 3B, lanes 1 and 2). By contrast, when cells were treated with Pur, Gli3FL became less abundant (Humke et al., 2010) (Fig. 3B, lane 3, Fig. 3C). However, in the GPR17-expressing cells, the change in Gli3FL was less than that of the control cells with Pur (Fig. 3B, lane 4, Fig. 3C), suggesting that the effect of Pur on Gli3 was perturbed by the presence of GPR17.

We further measured the cAMP levels in the cells, because modification of Gli3 proteins depends on the intracellular cAMP levels (Wang and Li, 2006). As a result, we found a higher cAMP level in GPR17-overexpressed cells than in control cells (Fig. 3D). Furthermore, a reporter assay measuring the activity of the cAMP-responsive element-binding region (CREB) revealed that the transfection of the *Gpr17* expression plasmid raised the CREB activity, confirming that the intracellular cAMP level was raised upon the overexpression of *Gpr17* (Fig. 3E). In cAMP-related assays (Fig. 3D,E), *Gpr161* was used as a positive control (Mukhopadhyay et al., 2013). Taken together, these findings demonstrated that GPR17 functions as a negative regulator of the Shh signalling pathway by upregulating the cAMP level.

GPR17 negatively regulates the ventral identity of the neural tube in a temporal manner

To investigate the activity of GPR17 in neural tube development and pattern formation, we overexpressed *Gpr17* by *in ovo* electroporation in the neural tube of the chick embryos, and monitored its effect on dorsal-ventral pattern formation. However, pattern formation was not significantly altered (Fig. S5A-C″). This could be because a trigger (i.e. a ligand) is necessary to activate GPR17-mediated signalling, and we speculated that the combination of GPR17 with its agonist,

Development (2019) 146, dev176784. doi:10.1242/dev.176784

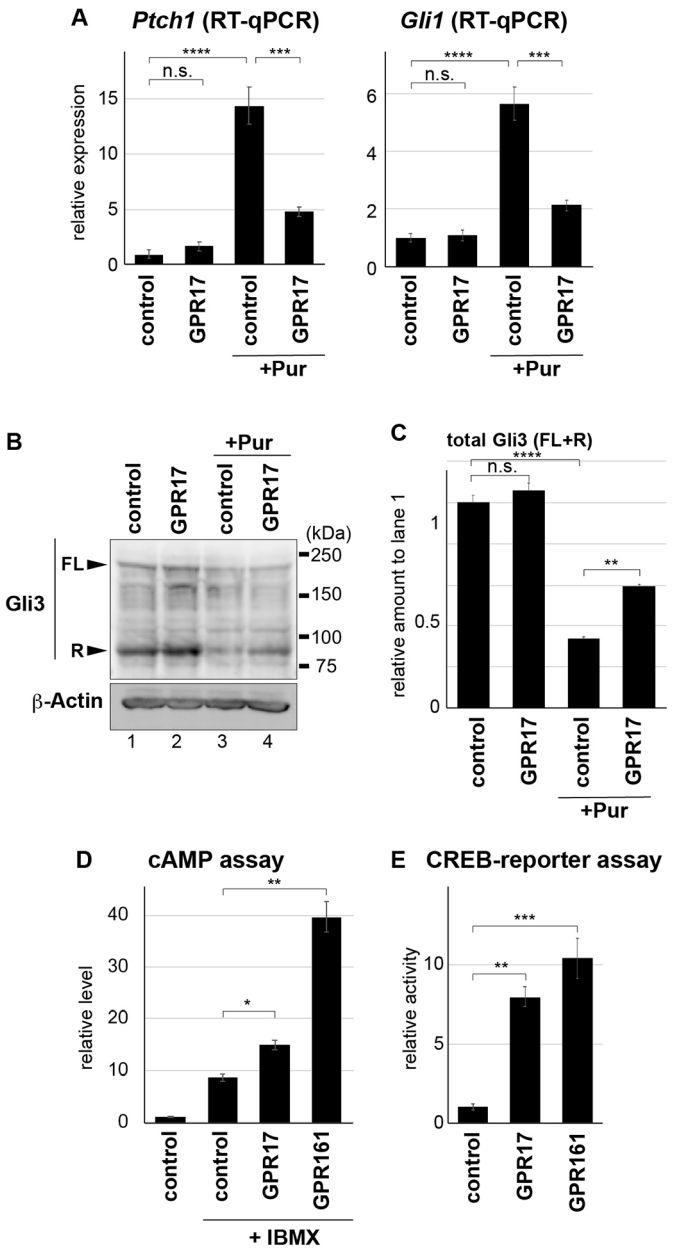

Fig. 3. GPR17 is a negative regulator for the Shh signalling pathway. (A) Overexpression of GPR17 decreased the expression levels of *Ptch1* and *Gli1* following Pur treatment. NIH3T3 cells transfected with or without indicated plasmids were treated with Pur for 24 h, and expression of *Ptch1* and *Gli1* was analysed by RT-qPCR. (B) The processing of Gli3 was altered in the *Gpr17*-transfected cells. Control (lanes 1 and 3) or *Gpr17* (lanes 2 and 4) expression plasmids were transfected into the NIH3T3 cells and cells were cultured with 500 nM of Pur for 6 h. The cell lysates were analysed by western blotting. (C) The quantitative data of the total Gli3FL and Gli3R from B. (D) The cAMP level is upregulated by GPR17. NIH3T3 cells were transfected with control or mouse *Gpr17* expression plasmids. Intracellular cAMP was measured. (E) The CREB activity was measured by a luciferase assay.

MDL29951 (Hennen et al., 2013), would embody the phenotype of the *Gpr17* overexpression.

To confirm that GPR17 and MDL29951 act synergistically, we administered a submaximal level of MDL29951 onto the embryos, and found that the neural tube patterning was not changed (Fig. S6A-C). By contrast, when MDL29951 was administered to the embryos in which GPR17 was overexpressed, the expression of Olig2 and Nkx2.2 was decreased in the electroporated cells, with the expansion of the dorsal marker Pax7 (Fig. S6D-F″). This finding suggests that GPR17 acts synergistically with MDL29951 in a cell-autonomous manner.

To find the effect of the GPR17-related signal in the dorsal-ventral patterning of the whole neural tube, we employed a new culture system, in which embryos were cultured *ex ovo* (Psychoyos and Finnell, 2008). The embryos were cultured in the absence or in the presence of an effective level of MDL29951. As a result, the ventral neural domains characterised by Olig2 and Nkx2.2 were significantly reduced (Fig. 4A-D), while the Pax7-expressing area was expanded (Fig. 4E,F), with the decreasing expression of *Ptch1* (Fig. 4G,H), suggesting that the ventral neural differentiation was abrogated. By contrast, FoxA2 and *Shh* expression was intact (Fig. 4I-L), suggesting that perturbation of the dorsal-ventral pattern has arisen by a change in the characteristics of the neural progenitor cells, rather than by alteration of the expression level of *Shh*.

Next, to reveal the relationship between the intracellular Shh signal and GPR17 more directly, we conducted an explant analysis. Because the expression of *Gpr17* is induced by Shh and GPR17 negatively regulates the Shh signal activity at the intracellular level (Figs 2G and 3A), we reasoned that GPR17 is involved in temporal regulation of Gli activity (Balaskas et al., 2012; Dessaud et al., 2010, 2007). To test this hypothesis, we measured the Gli activity over time. At 6 h, the Gli activity was comparable in the explants treated with Shh^{H} in the absence and presence of 30 µM of MDL29951 (Fig. 4M, lanes 1 and 2). However, at the 24 h time point, the explants added with MDL29951 along with Shh^{H} displayed a significantly reduced level of Gli activity than those without MDL29951 (Fig. 4M). These data suggest that the temporal Gli activity was perturbed by GPR17 and its related signals.

As the Gli activity was decreased in the Shh^{H} explants by MDL29951, we expected that the neural identities were also altered. Shh^{H} treatment of the explants for 24 h simulated the differentiation into ventral neural progenitor cells; Nkx2.2 expression was detectable in the majority of cells, and Olig2 in a smaller subset (Fig. 4N,P,R,T). By contrast, when the explants were treated with MDL29951 along with Shh^{H}, the number of cells expressing Nkx2.2 decreased, whereas Olig2-positive cells increased (Fig. 4O,Q,S,T). Given that the Olig2-expressing cells can be induced by a lower concentration of Shh (Dessaud et al., 2007), the results are consistent with those obtained from the measurement of Gli activity, and Shh was partially inhibited by the GPR17-associated signalling. This tendency was confirmed by using the Smo agonist Pur (500 nM), which induced a large number of Nkx2.2-positive cells. When used in combination with MDL29951, the numbers of Nkx2.2-positive cells decreased and Olig2-expressing cells instead increased (Fig. S6G-M). This result supports the idea that GPR17-related signal negatively regulates the effect of Shh.

Next, the same analyses were performed with the Shh^{L}-treated explants. As in the case of Shh^{H}, the Gli activity was comparable at 6 h (Fig. S6N). In addition, at 24 h, the activity in the MDL29951-treated Shh^{L} explants was at a similar level to those without MDL29951. Consistently, the assignment of the neural identities was not altered; Olig2-expressing cells dominated regardless of the MDL29951 treatment (Fig. S6O-U). Given that the Gli activity is downregulated quickly in Shh^{L} conditions (Dessaud et al., 2010, 2007), this result suggests that MDL29951 did not exert a significant blocking effect on the Shh^{L}, and the collective results

Development (2019) 146, dev176784. doi:10.1242/dev.176784

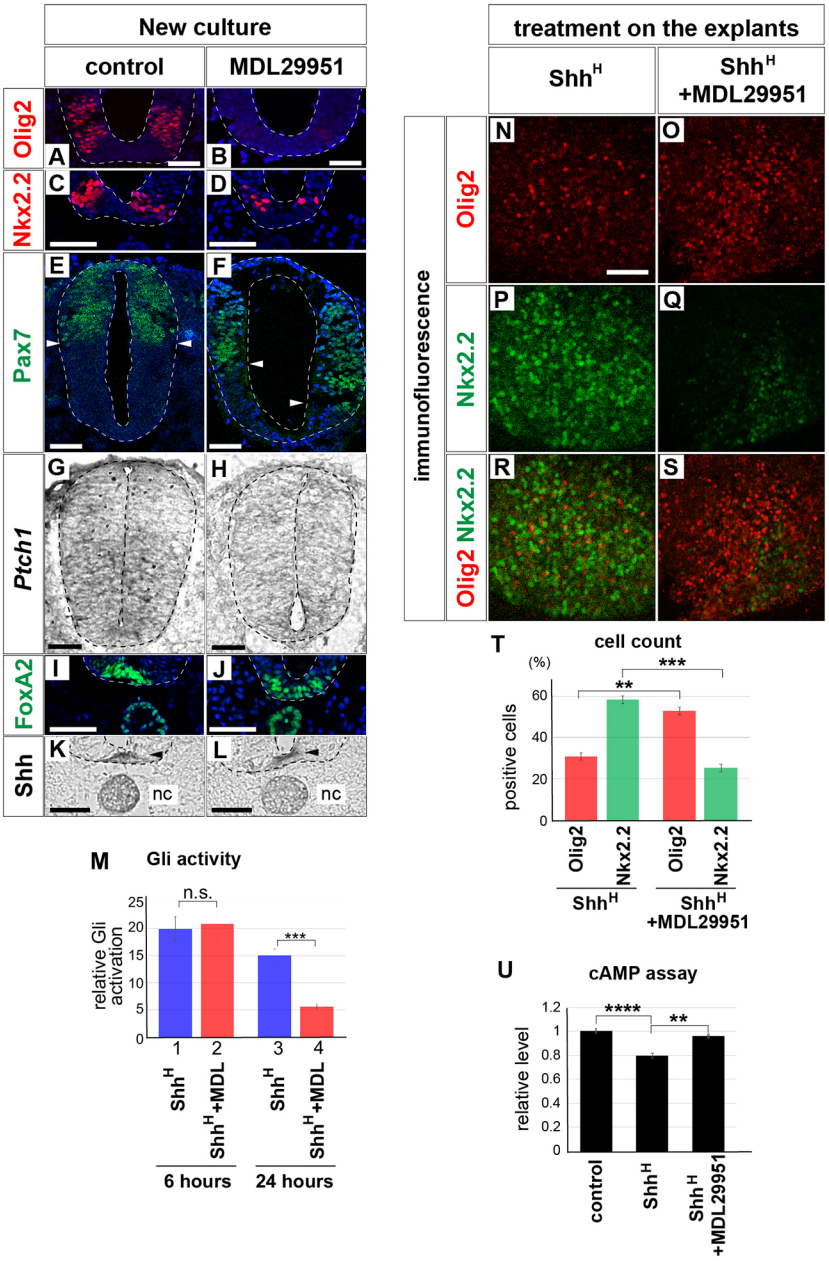

Fig. 4. GPR17 negatively regulates the Shh signalling pathway and affects the cell identity of neural progenitors. (A-L) The ventral identity was affected by MDL29951. The embryos were cultured using the New culture system with the control solvent (DMSO; A,C,E,G,I,K) or with 100 µM of MDL29951 (B,D,F,H,J,L) and the expression of Olig2 (A,B), Nkx2.2 (C,D), Pax7 (E,F), *Ptch1* (G,H), FoxA2 (I,J) and *Shh* (K,L) was analysed by immunofluorescence (A-F,I,J) or by *in situ* hybridisation (G,H,K,L). Ventral ends of the Pax7 expression are indicated by white arrowheads in E,F. The Shh expression is indicated by black arrowheads in K,L. nc, notochord. (M) The dynamic Gli activity is affected in the neural explants treated with Shh^H and MDL29951. Explants electroporated with *GBS-Luc* were treated with control medium, Shh^H or Shh^H+MDL29951 for 6 or 24 h. (N-T) Ventral identities are altered by treatment with MDL29951, a specific agonist of GPR17. Explants were incubated for 24 h with Shh^H in the absence (N,P,R) or presence (O,Q,S) of 30 µM MDL29951, and were stained using anti-Olig2 (N,O,R,S) and -Nkx2.2 (P,Q,R,S) antibodies. Quantification in given in T. (U) cAMP levels are upregulated by treatment with MDL29951 in the intermediate neural explants. Explants were prepared and treated with control, Shh^H or Shh^H+MDL29951 for 24 h. Scale bars: 50 µm.

above suggest that GPR17-related signal perturbed the Gli activity in a time-dependent manner.

It is unlikely that the alteration of the pattern formation is mediated by the programmed cell death, as a TdT-mediated dUTP nick end-labelling (TUNEL) assay also failed to detect a significantly increased number of positive signals in the explants (Fig. S7A-C).

We attempted to further investigate whether the activation of the GPR17-related signal correlated with the elevation of the intracellular cAMP level in the intermediate neural explants. Consistent with the previous observation (Hammerschmidt et al., 1996; Humke et al., 2010; Moore et al., 2016), the cAMP levels in the explants treated with Shh for 24 h showed a lower cAMP level than in the control explants (Fig. 4U, lanes 1 and 2). However, in the explants treated with MDL29951 in combination with Shh, this level was restored (Fig. 4U, lanes 1 and 3), suggesting that MDL29951 perturbed the Shh-mediated decrease in cAMP levels.

The regulation of cAMP levels by the GPR17-related signal occurred at upstream of PKA, because the ventralising effect induced by the dominant-negative PKA (dnPKA) could not be reverted by the coelectroporation with GPR17 followed by the administration of MDL29951, as confirmed by the expression of Nkx2.2 (Fig. S7D-E″). Together, these findings suggested that the GPR17-mediated signalling pathway negatively regulates Shh activity in the context of neural tube pattern formation through the upregulation of intracellular cAMP levels.

Inhibition of GPR17 expression causes aberrant expansion of ventral progenitor domains

To further investigate the functions of GPR17 in the development of neural tube pattern formation, we employed a loss-of-function approach. For this purpose, we designed two siRNAs targeting GPR17 (*si-Gpr17-1* and *si-Gpr17-2*), and carried out *in ovo* electroporation into the neural tube.

Development (2019) 146, dev176784. doi:10.1242/dev.176784

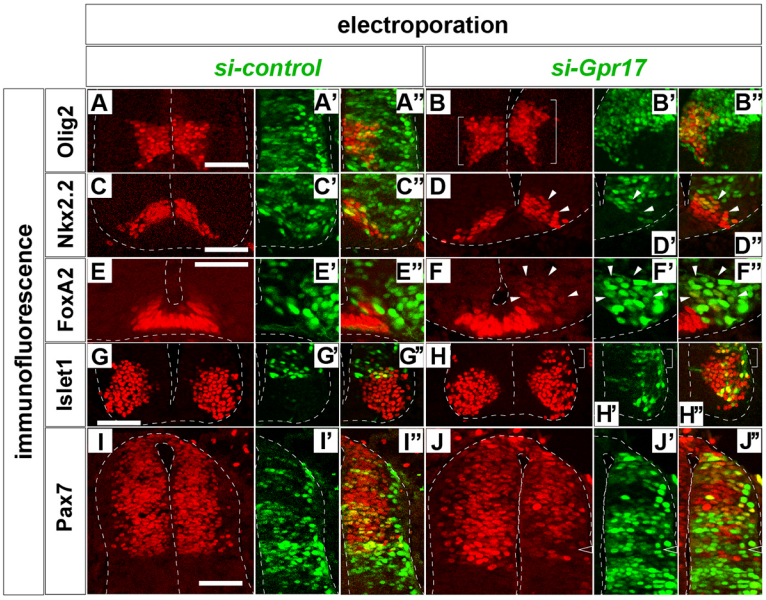

Fig. 5. Knockdown of *Gpr17* affects dorsal-ventral pattern formation of the neural tube. The neural tube was electroporated with *si-control* (A-A″,C-C″,E-E″,G-G″,I-I″) or *si-Gpr17* (B-B″,D-D″,F-F″,H-H″,J-J″) at HH stage 12 on the right side of the neural tube, and incubated for 48 h until the embryos reached HH stage 24. Sections of the neural tube were analysed with antibodies against Olig2 (A-B″), Nkx2.2 (C-D″), FoxA2 (E-F″), Islet1 (G-H″) or Pax7 (I-J″). Scale bars: 50 µm (bars in A,C,E,G and I apply to A-B″, C-D″, E-F″, G-H″ and I-J″, respectively). Expanded areas are indicated by brackets and white arrowheads, and reduced areas are outlined with arrowheads in J-J″.

We first electroporated *si-Gpr17* into the neural tube at HH stage 12. At 48 h post-treatment, we observed aberrant expansion of the ventral neural domains characterised by Olig2, Nkx2.2 and FoxA2 expression and of the motor neuron domain, identified by Islet1 expression (Fig. 5A-H″). Moreover, probably because the low level expression of *Gpr17* was perturbed by *si-Gpr17*, the area positive for Pax7 expressed in the dorsal progenitor domains was diminished (Fig. 5I-J″). This finding suggests that GPR17 per se is a negative regulator of Shh signal. This aberrant expression was abolished by co-electroporation of mouse *Gpr17*, which is not targeted by *si-Gpr17* (Fig. S5D-F″), suggesting that the phenotype observed in *si-Gpr17* transfection was due to downregulation of *Gpr17* expression. Furthermore, co-electroporation of *Gpr161*, another negative regulator of the Shh signalling pathway (Mukhopadhyay et al., 2013), did not abolish the phenotypes caused by *si-Gpr17*, confirming the specificity of *si-Gpr17* (Fig. S5G-I″). The expansion of ventral identity was also observed when *si-Gpr17-2* was electroporated into neural tubes (Fig. S8), validating the phenotype. Thus, GPR17 was demonstrated to be a negative regulator of the intracellular Shh signalling, and is essential for proper pattern formation in the neural tube.

GPR17 is essential for dynamic control of Shh activity

Finally, we investigated whether GPR17 plays an essential role for the temporal regulation of Gli activity (Balaskas et al., 2012; Dessaud et al., 2010, 2007). First, we asked whether the intracellular Shh signal activity was aberrantly upregulated by preparing intermediate neural explants electroporated with *si-Gpr17* then treating them with Shh^L. Although Olig2-expressing cells were predominant in the *si-control* electroporated explants (Fig. 6A-D,I), a significantly higher population of Nkx2.2-positive cells appeared at 24 h in the *si-Gpr17*-electroporated explants (Fig. 6E-H,I), suggesting that the intracellular Shh signal activity was upregulated when *Gpr17* expression was reduced. This observation was supported by the effect of treatment with pranlukast, a chemical antagonist of GPR17 (Hennen et al., 2013; Parravicini et al., 2010); explants treated with 10 µM pranlukast in combination with Shh^L tended to contain larger proportions of Nkx2.2-positive cells than controls, suggesting that perturbation of GPR17 caused the more ventral identity (Fig. S9A-G).

We next sought to analyse dynamic control of the intracellular Shh signal activity during ventral neural differentiation. To achieve this, we performed luciferase reporter assays using *GBS-Luc* at various time points. We prepared explants electroporated with *GBS-Luc* with either *si-control* or *si-Gpr17*, and then measured Gli activity at a series of time points from 6 to 48 h after the initiation of the culture. In *si-control*-electroporated explants treated with Shh^L, Shh activity gradually decreased over time, peaking at 6 h and becoming undetectable by the 48 h time point (Fig. 6J, blue line), consistent with previous reports (Dessaud et al., 2010, 2007). On the other hand, in explants with *si-Gpr17*, Gli activity at 6 h was comparable with that of the *si-control* explants, but the activity was significantly higher at 24 h and still detectable at 36 h (Fig. 6J, red line).

We next attempted to confirm that the dynamic Gli activity reflects the gene expression. We therefore cultured the explants electroporated with *si-control* or *si-Gpr17* in the presence of Shh^L for different time periods, and measured the expression levels of *Ptch1* and *Gli1* by RT-qPCR. As the result, the expression peaked at 12 h and then decreased quickly at 24 h in *si-control*-electroporated explants (Fig. 6K, Fig. S9H, blue lines). However, in the *si-Gpr17*-electroporated explants, although the expression at 12 h was comparable, the decrease was delayed and the expression level was significantly higher at 24 h (Fig. 6K, Fig. S9H, red lines). The successful perturbation of *Gpr17* expression was confirmed by RT-qPCR against the GPR17 primers (Fig. S9I). This result supports the idea that the dynamic Gli activity was affected by the perturbation of GPR17 expression.

We then asked whether the dynamic Gli activity corresponds to the processing of the Gli3 protein. For this, we performed western blots with the anti-Gli3 antibody in the chick explants electroporated with either *si-control* or *si-Gpr17*. At 6 h, the Gli3 protein processing was significantly affected by the treatment with Shh both in *si-control*- and *si-Gpr17*-transfected cells (Fig. 6L, left panel, Fig. 6M). By contrast, at 24 h, although the *si-Gpr17*-electroporated explants did not change the Gli3 processing in the absence of Shh (Fig. 6L, lanes 5 and 6, Fig. 6M), they contained significantly more destabilised Gli3 than did the *si-control* explants upon the treatment with Shh (Fig. 6L, lanes 7 and 8, Fig. 6M). This suggests that GPR17 affects the temporal processing of Gli3.

Development (2019) 146, dev176784. doi:10.1242/dev.176784

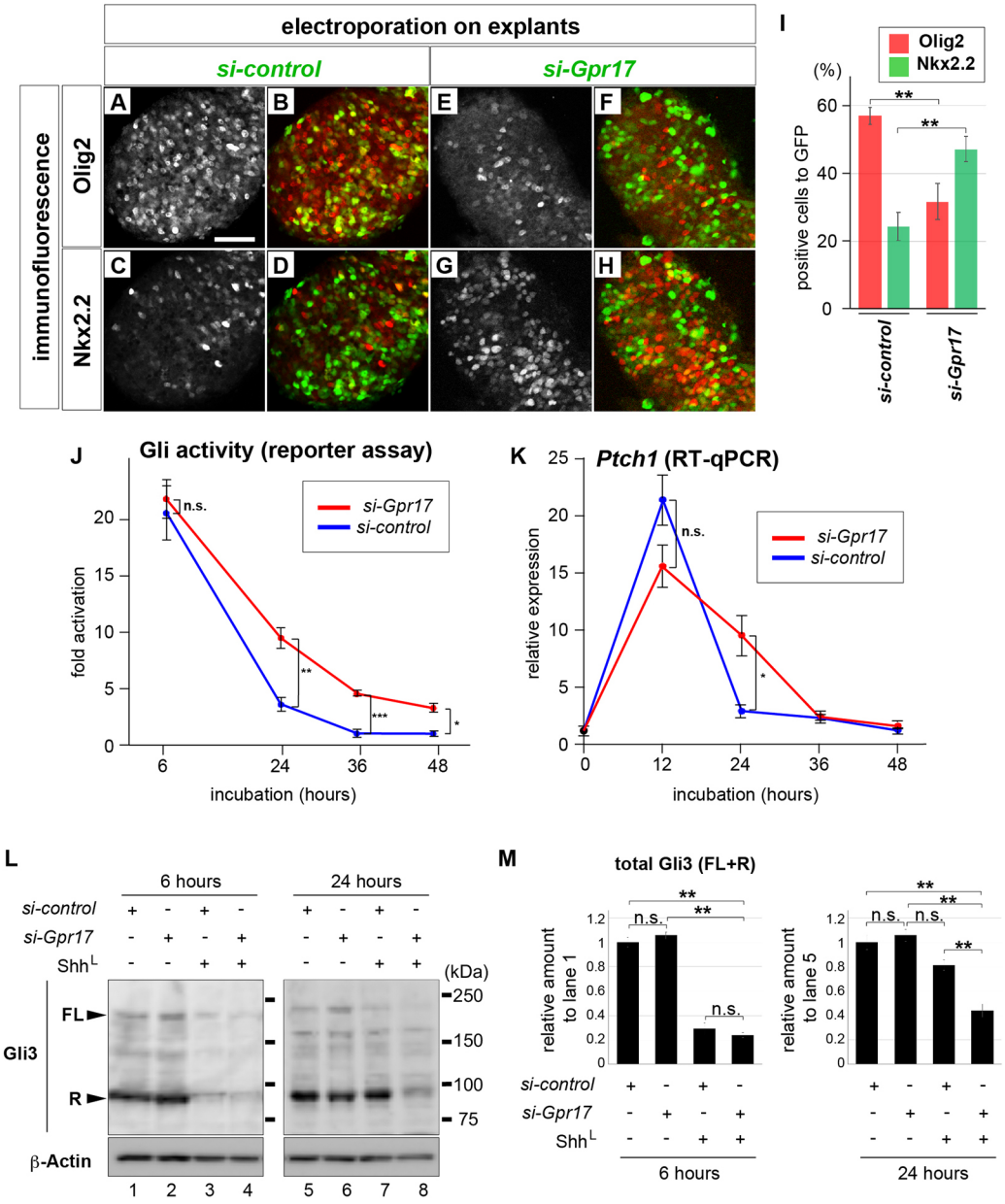

Fig. 6. GPR17 controls temporal Gli activity. (A-H) Knockdown of *Gpr17* induces more ventral identity. Intermediate neural explants electroporated with *si-control* (A-D) or *si-Gpr17* (E-H) were treated with Shh^{L} for 24 h, and expression was analysed with antibodies against Olig2 (A,B,E,F) or Nkx2.2 (C,D,G,H) and GFP (B,D,F,H). Scale bar: 50 µm. (I) Quantitative data for A-H. (J) Feedback of Gli activity is partially perturbed by knocking down GPR17. Explants electroporated with *si-control* (blue line) or *si-Gpr17* (red line) together with GBS-Luc were incubated with Shh^{L} at indicated time points and luciferase activity was measured. (K) Prolonged expression of *Ptch1* in the intermediate neural explants treated with Shh^{L}. *si-control*- (blue line) or *si-Gpr17*- (red line) electroporated explants were treated with Shh^{L} and the *Ptch1* mRNA levels were analysed in the samples harvested every 12 h. (L,M) Suppression of *Gpr17* expression changes the total amounts of the Gli3FL and Gli3R. Neural explants electroporated with either *si-control* or *si-Gpr17* were prepared and cultured for 6 h (left) and 24 h (right) in the absence (lanes 1, 2, 5 and 6) or in the presence (lanes 3, 4, 7 and 8) of Shh and were analysed by western blotting with the Gli3 antibody. (M) The total amounts of Gli3FL and Gli3R were quantified from four independent experiments.

Together, these findings indicate that GPR17 is an essential upstream factor that controls the dynamic change between the full-length and repressor forms of Gli3, and thus regulates the temporal change in intracellular Shh signalling activity.

GPR17 affects cell fate determination in neural differentiation from mouse ES cells

We finally assessed whether GPR17 functions are conserved in different organisms by investigating its functions in aspects of mouse development. For this analysis, we examined the directed neural differentiation of the ES cells, because the effects of treatments on gene expression are easily evaluated in this system. Mouse ES cells were differentiated into neural subtypes of pMN, p3 and floor plate using different combinations of retinoic acid (RA) and SAG, as described previously (Fig. S10A) (Kutejova et al., 2016). First, we evaluated GPR17 expression by RT-qPCR in each neural subtype. The results revealed significantly higher GPR17 expression in pMN and p3 cells than in FP 5 days after the start of differentiation (day 5) (Fig. 7A), suggesting that expression can be recapitulated in neural cells differentiated from ES cells.

Development (2019) 146, dev176784. doi:10.1242/dev.176784

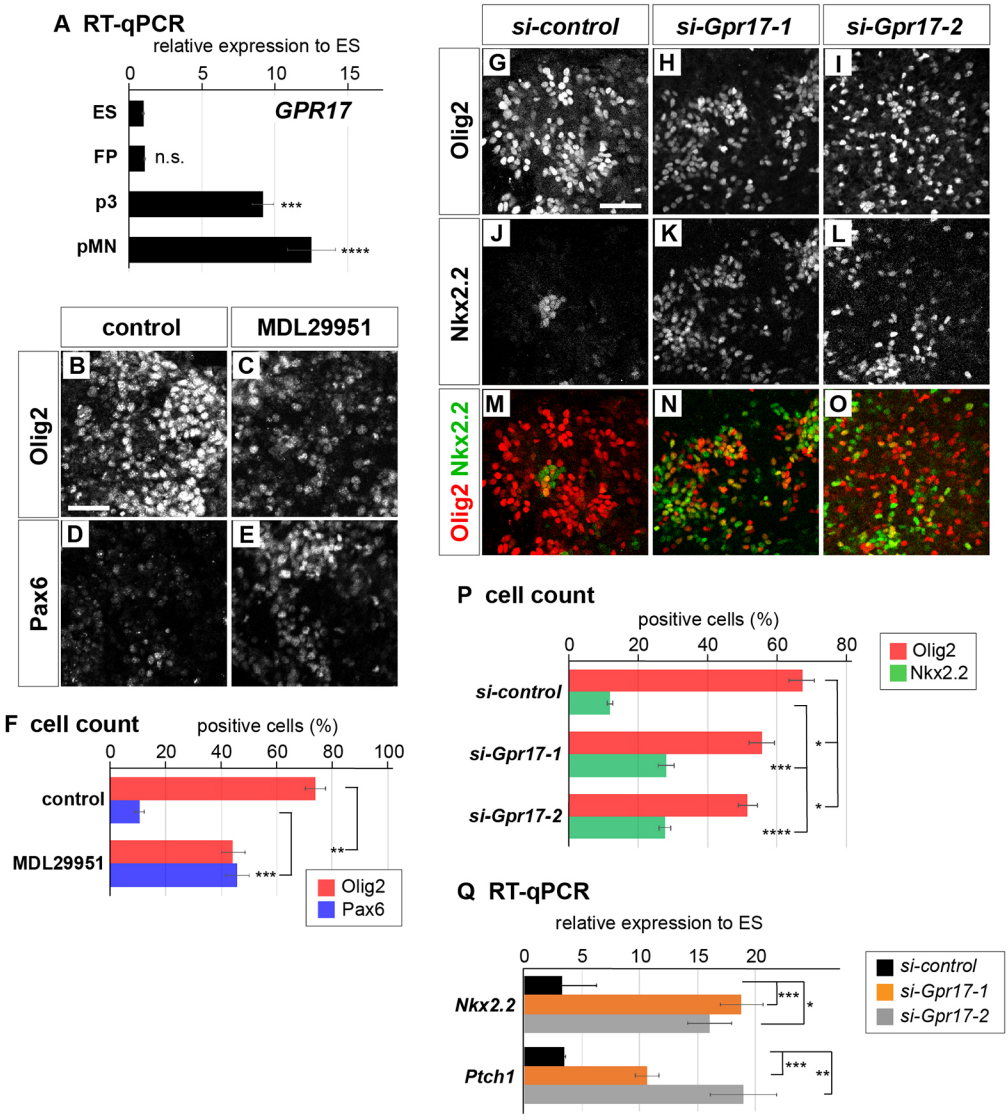

Fig. 7. GPR17 is required for proper directed neural differentiation from mouse embryonic stem cells. (A) GPR17 expression levels are subtype dependent. ES cells were differentiated according to the protocol in Fig. S8A, and the expression levels of *Gpr17* in each sample were analysed by RT-qPCR. (B-P) Directed neural differentiation from ES cells. (B-E) MDL29951 has a dorsalising effect on the neural fate. ES cells were differentiated according to the protocol shown in Fig. S8A, which mainly yields pMN cells. From day 3.5, DMSO (control; B,D) or 50 µM of MDL29951 (C,E) was added to the medium in addition to RA and Shh (as in the protocol). The cells were analysed using antibodies against Olig2 (B,D) and Pax6 (C,E). (F) Quantitative data for B-E. (G-O) Effects of *si-RNAs* targeting *Gpr17* for the neural fate determination. ES cells transfected with *si-control* (G,J,M), *si-Gpr17-1* (H,K,N) or *si-Gpr17-2* (I,L,O) were differentiated and analysed with antibodies against Olig2 (G-I) and Nkx2.2 (J-L) (M-O are merges). (P) Quantification of Olig2- and Nkx2.2-expressing cells over DAPI-positive cells. (Q) Expression levels of *Nkx2.2* and *Ptch1* were analysed by RT-qPCR. Scale bars: 50 µm.

By using this differentiation protocol, we analysed the effect of GPR17-related signal in the neural fate determination. During the differentiation into pMN, MDL29951 was added at day 3.5 and gene expression was evaluated at day 5.

In the pMN condition, the majority of cells expressed Olig2, with a small subset of Pax6-positive cells, as demonstrated by immunofluorescence (Fig. 7B,D,F). By contrast, the cells treated with MDL29951 displayed significantly larger numbers of Pax6-positive cells with reduced number of Olig2-positive cells (Fig. 7C,E,F), suggesting that the Shh signal was partially perturbed and cells obtained a more dorsal identity.

Conversely, we sought to analyse the essential function of GPR17 in neural differentiation and subtype determination, and transfected two different *si-RNAs* (*si-Gpr17-1* and *si-Gpr17-2*) targeting *Gpr17* in ES cells. The efficient knockdown of *Gpr17* expression was validated by RT-qPCR (three experiments; Fig. S10B).

Under these conditions, ES cells were differentiated into pMN cells, and gene expression was evaluated on day 5. In the pMN condition, the majority of cells expressed Olig2, with a small subset of Nkx2.2-positive cells, as demonstrated by immunofluorescence (Fig. 7G,J,M,P). By contrast, treatment with *si-Gpr17* increased the Nkx2.2-expressing cells (Fig. 7H,I,K,L,N-P). This observation suggests that *si-Gpr17*-treated cells became more susceptible to the Shh ligand and tended to differentiate into the more ventral identity of p3 (Fig. S10C-E), for which a higher level of Gli activity was required (Kutejova et al., 2016).

We next verified this tendency by RT-qPCR. In cells treated with *si-Gpr17s*, the *Nkx2.2* expression was higher than in *si-control*-transfected cells at day 5, confirming the results obtained by the immunofluorescence (Fig. 7Q). Furthermore, the expression level of *Ptch1*, a target gene of the Shh signal, was higher in *si-Gpr17* cells than in the controls (Fig. 7Q). These results were consistent with the findings obtained in the analyses of chick embryos. These findings suggest that mouse GPR17 is expressed in the pMN and p3 cells differentiated from ES cells, as in the chick embryos, and functions as a modulator for the ventral identities of the neural cells.

DISCUSSION

GPR17 is a negative regulator of the Shh signalling pathway and affects ventral pattern formation of the neural tube

In this study, we have demonstrated that the temporal change of the PKA activity in the neural progenitor cells confers the temporal adaptation against Shh (Fig. 1), and we isolated GPR17 as a modulator for this temporal activity (Fig. 3D,E,U). Although its

Development (2019) 146, dev176784. doi:10.1242/dev.176784

expression is induced by Shh, GPR17 negatively regulates the Shh signal, thereby affecting the dynamicity of the Gli activity (Dessaud et al., 2010, 2007). Negative regulation of the intracellular Shh signal by GPR17 is conserved in the mouse, as demonstrated by a system involving neural differentiation of ES cells (Fig. 7).

GPR17 was initially recognised as one of the genes that responds to neural tube injury, brain damage or pathological situations (Ceruti et al., 2009; Ciana et al., 2006; Lecca et al., 2008). A previous study using the mutant mice revealed that the deficiency of the *Gpr17* gene caused the earlier differentiation and excessive production of oligodendrocyte cells, suggesting that GPR17 determined the timing of oligodendrocyte differentiation (Chen et al., 2009). Subsequent studies have established the idea that GPR17 regulates the proliferation and differentiation of oligodendrocyte precursor cells (Lu et al., 2018; Merten et al., 2018). Given that oligodendrocyte differentiation is supported by Shh (Oh et al., 2005), the phenotypes caused by the alteration of the GPR17 expression may be mediated by the modulation of the Gli activity (Chen et al., 2009).

Although GPR17 has been suggested to be a receptor for the uracil nucleotides and cysteinyl leukotrienes (cysLTs) (Ciana et al., 2006; Fumagalli et al., 2016; Lecca et al., 2008), the actual ligand(s) that bind to GPR17 during development have not been identified. In this study, we used MDL29951 to experimentally activate GPR17 (Figs 4B,D,F,H,J,L,O,Q,S,U, S6A-F″,H,J,L,N,P,R,T, S7B). Although MDL29951 is recognised to be an agonist of GPR17 (Hennen et al., 2013) and has been used to analyse the function of GPR17 (Ou et al., 2016), it is also recognised as an antagonist of the N-methyl-D-aspartate (NMDA) receptor (Heppenstall and Fleetwood-Walker, 1997; Jansen and Dannhardt, 2003). However, as we demonstrated, MDL29951 synergistically acted with GPR17 at least in the context of the dorsal-ventral patterning (Fig. S4).

The *in vivo* functions of GPR17 in the mouse CNS development remain unknown but it seems that GPR17 is not crucial for the embryonic development (Chen et al., 2009; Lu et al., 2018; Merten et al., 2018), as *Gpr17*-deficient mice are viable. This is probably due to the redundant roles of the multiple factors expressed in the mouse neural tube. One such candidate is adenylyl cyclase 5 (AC5; *Acdy5*), which catalyses the dissociation of ATP to make cAMP (Moore et al., 2016; Vuolo et al., 2015). As we found that *Acdy5* expression was induced by Shh both in chick and mouse neural explants (Fig. S11), the regulatory mechanism of AC5 (and its related factor AC6) is similar to that of GPR17. It is possible that GPR17 and other factors work in concert with each other to regulate the temporal adaptation of Shh, and the dependency on each gene is species specific.

GPCRs can bind to different types of Gα proteins, including $G\alpha_i$, $G\alpha_s$, $G\alpha_q$ and $G\alpha_{12,13}$ (Rosenbaum et al., 2009). Among these Gα proteins, $G\alpha_q$ and $G\alpha_s$ can increase the intracellular cAMP level, whereas $G\alpha_i$ proteins mostly exert an inhibitory effect, and GPR17 can bind all types of G protein (Hennen et al., 2013). During the remyelination, GPR17 binds to $G\alpha_i$ and decreases the cAMP level (Buccioni et al., 2011; Ou et al., 2016; Parravicini et al., 2008; Simon et al., 2016). By contrast, in our experiments GPR17 instead upregulated cAMP levels (Fig. 2G), presumably by binding to $G\alpha_q$ and/or $G\alpha_s$, suggesting that it has diverse and cell type-specific functions.

GPR17 constitutes a negative-feedback loop of the Shh signalling system

A historical model suggested that a morphogen can produce a number of cell types depending on the thresholds of the signal concentration (Wolpert, 1969). This hypothesis relies on the supposition that signal concentration completely corresponds to the intracellular signal intensity. However, recent studies suggest that the temporal change in signal activity, so-called temporal adaptation, is crucial for cell fate determination and correct pattern formation (Dessaud et al., 2010, 2007; Ribes and Briscoe, 2009). The results of this study reveal a novel negative-feedback loop constructed by a GPCR through regulation of intracellular cAMP levels and processing of Gli transcription factors (Fig. 1). Recent mathematical modelling suggests the existence of negative regulators induced by Shh (Cohen et al., 2015), and our findings regarding GPR17 are in good agreement with this hypothesis.

The function of GPR17 is to modulate intracellular cAMP levels (Figs 3D and 4U). In this study, we analysed the processing of Gli3 to evaluate the Gli activity (Figs 1I, 3B and 6L) but Gli2 has been shown to play essential roles in the dorsal-ventral patterning of the neural tube (Pan et al., 2009). Therefore, the analysis on the dynamics of Gli2 processing may also be intriguing in a future study.

Although Shh induces the *Gpr17* expression (Fig. 2G), *Gpr17* does not seem to be a direct target gene of Gli transcription factors, as *GBS* has not been identified in the flanking regions of the *Gpr17* gene locus (Kutejova et al., 2016). Instead, Olig2 is the direct regulator of *Gpr17* expression (Ou et al., 2016). Consistent with this finding, overexpression of Olig2 in neural explants induces *Gpr17* expression (Fig. 2H). This could explain why the negative-feedback regulation is cell type-specific and does not take place in the NIH3T3 cells treated with the Shh ligand (Cohen et al., 2015); Olig2 expression is induced only in the neural progenitor cells, but not in NIH3T3 cells (A.Y., A.H. and N.S., unpublished).

In a developmental context, negative-feedback regulation confers diversity of cell types and robustness of pattern formation (Dessaud et al., 2010). To date, multiple negative-feedback systems for Gli activity have been identified (Cohen et al., 2015). For example, the *Ptch1* gene, the product of which negatively regulates the intracellular Shh signal activity, is a direct target of Shh (Fig. 8) (Dessaud et al., 2007). Moreover, expression of the transcriptional mediator Gli2 decreases over time during neural development, although the underlying regulatory mechanisms remain elusive (Cohen et al., 2015). In combination with the existence of GPR17,

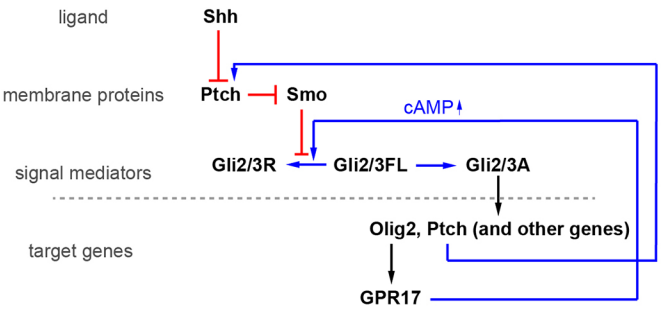

Fig. 8. A working model for the negative regulation of the intracellular Shh signalling pathway. The binding of Shh (ligand) to Ptch1 (a membrane protein) abrogates its repressive effect on Smo, and the conversion from the full-length forms (Gli2/3FL) to their repressor forms (Gli2/3R) is thereby perturbed. Gli2/3FL are further modified to their active forms (Gli2/3A) and are translocated to the nucleus where the target genes, including *Olig2* and *Ptch1*, are induced. It has been shown that the accumulation of *Ptch1* transcript results in the perturbation of the Shh signal transduction. In addition, as demonstrated in our study, Olig2 induces the *Gpr17* gene expression, and the upregulation of cAMP encourages the accumulation of Gli2/3R. The positive and negative regulations are indicated by blue and red lines, respectively. The transcriptional regulation is indicated by black lines.

Development (2019) 146, dev176784. doi:10.1242/dev.176784

as this study demonstrated (Fig. 8), multiple negative-feedback systems could cause differences in the half-life of the signal in each progenitor cell, allowing diverse cell types to be produced by a single morphogen, Shh. Moreover, during formation of the morphogen gradient, uncertainties and fluctuations may arise. This noise in the signal is constantly modulated by negative feedback, and consequently the reliability and reproducibility of pattern formation can be established (Lander, 2011; Perrimon et al., 2012). Therefore, the negative-feedback loop formed by Shh and GPR17 is important not only for overall neural tube pattern formation, but also for fine tuning of signal intensity; consequently, it establishes the quantitative balance among different cell types during neural and neuronal differentiation. Further studies, including analysis of the temporal change of intracellular cAMP levels, will reveal the significance of GPR17 in modulating the Shh signal using negative feedback.

MATERIALS AND METHODS

Isolation of GPR17

GPCRs that can couple with $G\alpha_q$ or $G\alpha_s$ were identified by referring to GPCRdb (gpcrdb.org); and qPCR primers were designed against the corresponding genes (Table S1). Relative expression levels were analysed by RT-qPCR in neural explants treated or untreated with Shh^H (Fig. S1). NCBI gene IDs for chicken and mouse *Gpr17* are 769024 and 574402, respectively.

Embryos, electroporation and expression analysis

All animal experiments were performed with the approval of the Animal Welfare and Ethical Review Panel of Nara Institute of Science and Technology (approval numbers 1636 and 1810 for chicken and mouse experiments, respectively). Chicken eggs were purchased from the Shiroyama Kei-en farm (Kanagawa prefecture, Japan) and the Yamagishi farm (Wakayama prefecture, Japan), and the developmental stages were evaluated using Hamburger and Hamilton's criteria (Hamburger and Hamilton, 1992). *In ovo* electroporation of chick embryos was carried out with an ECM830 electroporator (BTX), and embryos were incubated at 38°C for the indicated times. Overexpression in the chick embryos was performed with the constructs subcloned into the *pCIG* expression plasmid, which contains an IRES (internal ribosomal entry site) -GFP gene downstream of the gene of interest (Megason and McMahon, 2002). *pCIG-Olig2^{DBD}-VP16* was constructed by fusing the DNA-binding region of Olig2 with the transactivation domain of the viral protein VP16, as described previously (Zhou and Anderson, 2002; Zhou et al., 2001). Embryos were fixed with 4% paraformaldehyde, subsequently incubated with 15% sucrose for cryoprotection and embedded in 7.5% gelatine (Sigma). Cryosections were cut at 14 µm increments and analysed using immunofluorescence or *in situ* hybridisation. The sections from at least seven independent embryos were analysed, and the number of the embryos analysed is indicated in Table S2. For loss-of-function experiments, *si-cGpr17-1* [GGAACAGAGUGGAGAAACACCUG(dA)(dA) (sense) and UUCAGGUGUUUCUCCACUCUGUUCCCA (antisense)] or its negative control *si-control* [AUGCUUCUCCGAACGUGUCACGU(dT)(dT) (sense) and UUUCGUGACACGUUCGGAGAAGCAUCA (antisense); Eurofin] and *si-cGpr17-2* (CAGACUGUGGAAGUGAACAACACAA) or *si-control-2* (siRNA Negative Control, Med GC; Invitrogen) was electroporated with the *pCIG* vector, which encodes *GFP* as a tracer. Unless mentioned otherwise, loss-of-function experiments were performed with *si-cGpr17-1*. DIG-labelled (Roche) complementary RNA probe was synthesised using RNA polymerase (Promega). *In situ* hybridisation on slides was performed as described previously (Sasai et al., 2014).

Immunofluorescence was performed as described previously (Sasai et al., 2014). Primary antibodies against the following proteins were used in this study: Olig2 (rabbit, Millipore AB9610), Nkx2.2 (mouse, DSHB 74.5A5; rabbit, Abcam ab19077), Islet1/2 (DSHB 39.4D5), Pax7 (DSHB), FoxA2 (goat, Santa Cruz sc-6554X), Sox2 (rabbit, Millipore AB5603), GPR17 (goat, Abcam ab106781 for mouse embryos; rabbit, Sigma SAB4501250 for cells), GFP (sheep, AbD Serotec 4745-1051), Gli3 (goat, R&D AF3690), β-Actin (rabbit, Abcam ab8227) and γ-acetylated tubulin (mouse, Sigma T7451). For GPR17 immunofluorescence in mouse embryonic sections, antigenic retrieval was required; slides were boiled for 1 min in 10 mM citric acid (pH 6.0) solution prior to the incubation with the primary antibody. Fluorophore- and HRP-conjugated secondary antibodies were purchased from Jackson Laboratory and Cell Signaling Technology, respectively.

New culture and intermediate neural explants

New culture was performed as described previously (Psychoyos and Finnell, 2008). Culture plates containing albumen and agarose were prepared with the final concentration of 100 µM of MDL29951 or with dimethylsulfoxide (DMSO) (control). Chick embryos were taken from the eggs at HH stage 12 with a ring of filter paper, and put on the culture plates with the ventral side up. Embryos were cultured in the 38°C incubator for 36 h, and the plates were kept humid with Hanks' Balanced Salt solution (1×HBSS; Sigma-Aldrich).

Chick intermediate neural explants were prepared as described previously (Sasai et al., 2014). HH stage 9 embryos were isolated from the eggs and maintained in L-15 medium (Thermo Fisher Scientific). After treatment with Dispase II (Sigma), the intermediate region of the neural plate at the preneural tube level (Delfino-Machin et al., 2005) was manually excised from the embryos and cultured in DMEM/F-12 medium (Thermo Fisher Scientific) supplemented with Mito+Serum Extender (Sigma) and penicillin/streptomycin/glutamine (Wako). The explants were cultured in the pH-adjusted collagen gel (Sigma; for immunofluorescence and RT-qPCR) or on the glass plates coated with gelatin (Sigma; for western blots). Quantitation of positive cells was performed in at least five areas, each of which contained ∼200-250 cells, randomly chosen from independent explants. Shh^L and Shh^H were defined as the concentrations of Shh that differentiate explants into motor neuron and floor plate at 48 h, respectively (Fig. S1). Shh^H is four times as high as Shh^L. H-89 (Wako) and MDL29951 were used at the indicated concentrations. For RT-qPCR analyses, RNA was extracted from the pools of 15 chick intermediate neural explants by using PicoPure RNA extraction kit (Thermo Fisher Scientific). Each extraction produced a range of 500 ng (12-h culture) to 1.5 µg (48-h culture) of total RNA, as measured by Nanodrop (Thermo Fisher Scientific). Complementary DNAs (cDNAs) were synthesised by PrimeScript reverse transcriptase (TaKaRa), and qPCR was performed by using LightCycler 96 (Roche). At least two independent pools of explants were analysed in each experiment, and each gene expression level was normalised to the *Gapdh* expression. Mouse neural explants (Fig. S11) were prepared from the E8.5 embryos and were cultured in the same way as in the chick explants (Balaskas et al., 2012), except that the culture medium contained N2 and B27 supplements (Thermo Fisher Scientific).

Cell culture, transfection and selection

NIH3T3 fibroblast cells were maintained in Dulbecco's modified Eagle's medium /F12 medium (Wako) containing 10% New-Born Calf Serum (MP Biomedicals). Lipofectamine 3000 (Invitrogen) was used for transfection. To obtain explicit evidence of the effects on the overexpression of the genes in Fig. 3E-I, the transfected cells were selected for 48 h with 500 µg/ml of G418 (Invitrogen) from 1 day after the *pcDNA3*-based expression plasmids were transfected and used for assays.

Monitoring the Gli activity and the intracellular cAMP levels

The *GBS-Nano-Luc* reporter construct containing the *GBS* was constructed by subcloning of the octameric *GBS* (Sasaki et al., 1999) to the pNL3.2 vector (Promega) and used to monitor Gli activity. *pCS2-firefly luciferase* was used as an internal control. For the luciferase assays on chick neural explants, *GBS-Nano-Luc* and *pCS2-firefly-luciferase* were electroporated at the preneural tube region of the caudal part of the chick embryos at HH stage 9− (Delfino-Machin et al., 2005). *si-RNAs* were co-electroporated if necessary. The explants were then prepared and cultured under the indicated conditions. The relative luciferase activities were compared with those

Development (2019) 146, dev176784. doi:10.1242/dev.176784

cultured without Shh at every time point. Seven or eight explants were grouped for each measurement, and four to 10 groups of explants were measured per condition.

CREB-Luc (luciferase gene driven by the cAMP-responsive element-binding region) was a kind gift from Prof. Itoh (Nara Institute of Science and Technology, Ikoma, Japan) (Jenie et al., 2013) and *pRL-CMV* (Promega) was used for an internal control. The measurement of the chemiluminescence was performed by using the plate reader Tristar2 (Berthold Technologies).

For the cAMP assay in the NIH3T3 cells (Fig. 3D), the cells were transfected with the indicated plasmids and the transfected cells were selected for 24 h. 3-Isobutyl-1-methylxanthine (IBMX), a non-competitive selective phosphodiesterase inhibitor, was added at 1 µM in the final 30 min before cells were harvested to raise the basal level of intracellular cAMP. For the cAMP assay in the neural explants (Fig. 4U), 15 explants were prepared for each condition and cultured for 24 h. IBMX was added in the last 1 h. The cAMP assay was performed using DetectX high sensitivity direct cAMP Chemiluminescent Immunoassay Kit (Arbor Assays). The protein concentrations of the cell lysates were measured by CBB protein assay solution (Nacalai, Japan) and the measurement values were normalised.

TUNEL assay

TUNEL assay was performed to detect the apoptotic cells. The explants were incubated with TdT transferase (Roche) and DIG-labelled dUTP (Merck Millipore), and the signals were visualised using anti-digoxigenin-rhodamine antibody (Sigma). Staurosporine (Belmokhtar et al., 2001) was used as a positive control at 1 nM.

Neural differentiation of mouse ES cells

The Sox1-GFP ES cell line was kindly provided by Prof. Smith (University of Cambridge, UK), and maintenance and neural differentiation as a monolayer culture were performed as described previously (Kamiya et al., 2011; Kutejova et al., 2016; Ying et al., 2003). Briefly, on the fibronectin/collagen-coated plates, ∼1.5×10^4 ES cells were seeded and cultured as monolayers in the differentiation medium (Kutejova et al., 2016) for the initial 3 days. For pMN differentiation, 300 nM RA (Sigma) was added on day 3.0 and 50 nM SAG was added on day 3.5, and the cells were incubated for a total of 5 days. For p3 differentiation, 30 nM RA and 500 nM SAG (Sigma) were added on day 3.0 and day 3.5, respectively. For FP differentiation, 500 nM SAG was added on day 3.0. Before differentiation was initiated, Stealth *siRNAs* (Invitrogen) (*si-mGpr17-1*, UCGCCUGCUUCUACCUUCUGGACUU; *si-mGpr17-2*, ACCGUUCAGUCUAUGUGCUUCACUA) or *si-control* (Invitrogen) were transfected twice at 24 h intervals using Lipofectamine RNAiMAX (Invitrogen). For RT-qPCR analysis, RNA was extracted by RNeasy RNA extraction kit (QIAGEN). cDNA synthesis and qPCR were performed as in the chick neural explants.

Images and data analysis

Images were collected by using an AxioVision2 microscope (for *in situ* hybridisation images; Zeiss), a LSM 710 confocal microscope (for immunofluorescence data; Zeiss) and a LAS4000 ImageQuant (for western blots; GE Healthcare). Signal intensities of the western blots were calculated by ImageJ. Images were processed using Photoshop (Adobe) and figures were arranged on Illustrator (Adobe). Statistical analysis was performed using Prism (GraphPad) with two-tailed *t*-test (Figs 1J, 2H, 3A,C,D, 4M,T, 6I-K and 7F,P,Q) or with one-way analysis of variance (ANOVA) followed by Tukey's post-hoc test (Figs 1H,J, 2I, 3E, 4U, 6M and 7A). Data are presented as mean±s.e.m. and significance (*P<0.05, **P<0.01, ***P<0.001, ****P<0.0001; n.s., not significant) is indicated in each graph.

Acknowledgements

The authors are grateful to Profs Austin Smith and Hiroshi Itoh for materials; to Dr James Briscoe for comments on the manuscript; to Prof. Naoyuki Inagaki, and Drs Yuichi Sakumura and Takunori Minegishi for advice; to Prof. Takashi Toda for encouragement; and to all laboratory members for support and valuable discussion.

Competing interests

The authors declare no competing or financial interests.

Author contributions

Conceptualization: N.S.; Methodology: N.S.; Validation: N.S.; Formal analysis: A.Y., A.H., M.K., N.S.; Investigation: A.Y., A.H., M.K., N.S.; Resources: M.M.-T., T.K., N.S.; Data curation: A.Y., A.H., M.K., N.S.; Writing - original draft: N.S.; Writing - review & editing: N.S., A.Y.; Visualization: A.Y., N.S.; Supervision: N.S.; Project administration: N.S.; Funding acquisition: N.S., A.H.

Funding

This study was supported in part by Grants-in-Aid from the Japan Society for Promotion of Science (15H06411 and 17H03684 to N.S.) and from the Ministry of Education, Science and Technology, Japan (19H04781 to N.S.); by the Joint Research Program of the Institute for Genetic Medicine, Hokkaido University (T.K., N.S.); by the Takeda Science Foundation (N.S., A.H.); by the Mochida Memorial Foundation for Medical and Pharmaceutical Research (N.S.); by the Ichiro Kanehara Foundation for the Promotion of Medical Sciences and Medical Care (N.S.); by the Uehara Memorial Foundation (N.S.); and by the Novartis Foundation (Japan) for the Promotion of Science (N.S.).

Supplementary information

Supplementary information available online at
http://dev.biologists.org/lookup/doi/10.1242/dev.176784.supplemental

References

Balaskas, N., Ribeiro, A., Panovska, J., Dessaud, E., Sasai, N., Page, K. M., Briscoe, J. and Ribes, V. (2012). Gene regulatory logic for reading the Sonic Hedgehog signaling gradient in the vertebrate neural tube. *Cell* **148**, 273-284. doi:10.1016/j.cell.2011.10.047

Belmokhtar, C. A., Hillion, J. and Ségal-Bendirdjian, E. (2001). Staurosporine induces apoptosis through both caspase-dependent and caspase-independent mechanisms. *Oncogene* **20**, 3354-3362. doi:10.1038/sj.onc.1204436

Briscoe, J. (2006). Agonizing hedgehog. *Nat. Chem. Biol.* **2**, 10-11. doi:10.1038/nchembio0106-10

Briscoe, J., Sussel, L., Serup, P., Hartigan-O'Connor, D., Jessell, T. M., Rubenstein, J. L. R. and Ericson, J. (1999). Homeobox gene Nkx2.2 and specification of neuronal identity by graded Sonic hedgehog signalling. *Nature* **398**, 622-627. doi:10.1038/19315

Buccioni, M., Marucci, G., Dal Ben, D., Giacobbe, D., Lambertucci, C., Soverchia, L., Thomas, A., Volpini, R. and Cristalli, G. (2011). Innovative functional cAMP assay for studying G protein-coupled receptors: application to the pharmacological characterization of GPR17. *Purinergic Signal.* **7**, 463-468. doi:10.1007/s11302-011-9245-8

Ceruti, S., Villa, G., Genovese, T., Mazzon, E., Longhi, R., Rosa, P., Bramanti, P., Cuzzocrea, S. and Abbracchio, M. P. (2009). The P2Y-like receptor GPR17 as a sensor of damage and a new potential target in spinal cord injury. *Brain* **132**, 2206-2218. doi:10.1093/brain/awp147

Chen, Y., Wu, H., Wang, S., Koito, H., Li, J., Ye, F., Hoang, J., Escobar, S. S., Gow, A., Arnett, H. A. et al. (2009). The oligodendrocyte-specific G protein-coupled receptor GPR17 is a cell-intrinsic timer of myelination. *Nat. Neurosci.* **12**, 1398-1406. doi:10.1038/nn.2410

Ciana, P., Fumagalli, M., Trincavelli, M. L., Verderio, C., Rosa, P., Lecca, D., Ferrario, S., Parravicini, C., Capra, V., Gelosa, P. et al. (2006). The orphan receptor GPR17 identified as a new dual uracil nucleotides/cysteinyl-leukotrienes receptor. *EMBO J.* **25**, 4615-4627. doi:10.1038/sj.emboj.7601341

Cohen, M., Kicheva, A., Ribeiro, A., Blassberg, R., Page, K. M., Barnes, C. P. and Briscoe, J. (2015). Ptch1 and Gli regulate Shh signalling dynamics via multiple mechanisms. *Nat. Commun.* **6**, 6709. doi:10.1038/ncomms7709

Delfino-Machin, M., Lunn, J. S., Breitkreuz, D. N., Akai, J. and Storey, K. G. (2005). Specification and maintenance of the spinal cord stem zone. *Development* **132**, 4273-4283. doi:10.1242/dev.02009

Dessaud, E., Yang, L. L., Hill, K., Cox, B., Ulloa, F., Ribeiro, A., Mynett, A., Novitch, B. G. and Briscoe, J. (2007). Interpretation of the sonic hedgehog morphogen gradient by a temporal adaptation mechanism. *Nature* **450**, 717-720. doi:10.1038/nature06347

Dessaud, E., McMahon, A. P. and Briscoe, J. (2008). Pattern formation in the vertebrate neural tube: a sonic hedgehog morphogen-regulated transcriptional network. *Development* **135**, 2489-2503. doi:10.1242/dev.009324

Dessaud, E., Ribes, V., Balaskas, N., Yang, L. L., Pierani, A., Kicheva, A., Novitch, B. G., Briscoe, J. and Sasai, N. (2010). Dynamic assignment and maintenance of positional identity in the ventral neural tube by the morphogen sonic hedgehog. *PLoS Biol.* **8**, e1000382. doi:10.1371/journal.pbio.1000382

Epstein, D. J., Marti, E., Scott, M. P. and McMahon, A. P. (1996). Antagonizing cAMP-dependent protein kinase A in the dorsal CNS activates a conserved Sonic hedgehog signaling pathway. *Development* **122**, 2885-2894.

Fumagalli, M., Lecca, D. and Abbracchio, M. P. (2016). CNS remyelination as a novel reparative approach to neurodegenerative diseases: the roles of purinergic

signaling and the P2Y-like receptor GPR17. *Neuropharmacology* **104**, 82-93. doi:10.1016/j.neuropharm.2015.10.005

Hamburger, V. and Hamilton, H. L. (1992). A series of normal stages in the development of the chick embryo. 1951. *Dev. Dyn.* **195**, 231-272. doi:10.1002/aja.1001950404

Hammerschmidt, M., Bitgood, M. J. and McMahon, A. P. (1996). Protein kinase A is a common negative regulator of Hedgehog signaling in the vertebrate embryo. *Genes Dev.* **10**, 647-658. doi:10.1101/gad.10.6.647

Hennen, S., Wang, H., Peters, L., Merten, N., Simon, K., Spinrath, A., Blattermann, S., Akkari, R., Schrage, R., Schroder, R. et al. (2013). Decoding signaling and function of the orphan G protein-coupled receptor GPR17 with a small-molecule agonist. *Sci. Signal.* **6**, ra93. doi:10.1126/scisignal.2004350

Heppenstall, P. A. and Fleetwood-Walker, S. M. (1997). The glycine site of the NMDA receptor contributes to neurokinin1 receptor agonist facilitation of NMDA receptor agonist-evoked activity in rat dorsal horn neurons. *Brain Res.* **744**, 235-245. doi:10.1016/S0006-8993(96)01065-7

Holz, A., Kollmus, H., Ryge, J., Niederkofler, V., Dias, J., Ericson, J., Stoeckli, E. T., Kiehn, O. and Arnold, H.-H. (2010). The transcription factors Nkx2.2 and Nkx2.9 play a novel role in floor plate development and commissural axon guidance. *Development* **137**, 4249-4260. doi:10.1242/dev.053819

Humke, E. W., Dorn, K. V., Milenkovic, L., Scott, M. P. and Rohatgi, R. (2010). The output of Hedgehog signaling is controlled by the dynamic association between Suppressor of Fused and the Gli proteins. *Genes Dev.* **24**, 670-682. doi:10.1101/gad.1902910

Jansen, M. and Dannhardt, G. (2003). Antagonists and agonists at the glycine site of the NMDA receptor for therapeutic interventions. *Eur. J. Med. Chem.* **38**, 661-670. doi:10.1016/S0223-5234(03)00113-2

Jenie, R. I., Nishimura, M., Fujino, M., Nakaya, M., Mizuno, N., Tago, K., Kurose, H. and Itoh, H. (2013). Increased ubiquitination and the crosstalk of G protein signaling in cardiac myocytes: involvement of Ric-8B in Gs suppression by Gq signal. *Genes Cells* **18**, 1095-1106. doi:10.1111/gtc.12099

Kamiya, D., Banno, S., Sasai, N., Ohgushi, M., Inomata, H., Watanabe, K., Kawada, M., Yakura, R., Kiyonari, H., Nakao, K. et al. (2011). Intrinsic transition of embryonic stem-cell differentiation into neural progenitors. *Nature* **470**, 503-509. doi:10.1038/nature09726

Kutejova, E., Sasai, N., Shah, A., Gouti, M. and Briscoe, J. (2016). Neural progenitors adopt specific identities by directly repressing all alternative progenitor transcriptional programs. *Dev. Cell* **36**, 639-653. doi:10.1016/j.devcel.2016.02.013

Lander, A. D. (2011). Pattern, growth, and control. *Cell* **144**, 955-969. doi:10.1016/j.cell.2011.03.009

Le Dréau, G. and Martí, E. (2012). Dorsal-ventral patterning of the neural tube: a tale of three signals. *Dev. Neurobiol.* **72**, 1471-1481. doi:10.1002/dneu.22015

Lecca, D., Trincavelli, M. L., Gelosa, P., Sironi, L., Ciana, P., Fumagalli, M., Villa, G., Verderio, C., Grumelli, C., Guerrini, U. et al. (2008). The recently identified P2Y-like receptor GPR17 is a sensor of brain damage and a new target for brain repair. *PLoS ONE* **3**, e3579. doi:10.1371/journal.pone.0003579

Litingtung, Y. and Chiang, C. (2000). Specification of ventral neuron types is mediated by an antagonistic interaction between Shh and Gli3. *Nat. Neurosci.* **3**, 979-985. doi:10.1038/79916

Lu, Q. R., Yuk, D., Alberta, J. A., Zhu, Z., Pawlitzky, I., Chan, J., McMahon, A. P., Stiles, C. D. and Rowitch, D. H. (2000). Sonic hedgehog–regulated oligodendrocyte lineage genes encoding bHLH proteins in the mammalian central nervous system. *Neuron* **25**, 317-329. doi:10.1016/S0896-6273(00)80897-1

Lu, C., Dong, L., Zhou, H., Li, Q., Huang, G., Bai, S. J. and Liao, L. (2018). G-protein-coupled receptor Gpr17 regulates oligodendrocyte differentiation in response to lysolecithin-induced demyelination. *Sci. Rep.* **8**, 4502. doi:10.1038/s41598-018-22452-0

Megason, S. G. and McMahon, A. P. (2002). A mitogen gradient of dorsal midline Wnts organizes growth in the CNS. *Development* **129**, 2087-2098.

Merten, N., Fischer, J., Simon, K., Zhang, L., Schröder, R., Peters, L., Letombe, A.-G., Hennen, S., Schrage, R., Bödefeld, T. et al. (2018). Repurposing HAMI3379 to block GPR17 and promote rodent and human oligodendrocyte differentiation. *Cell Chem. Biol.* **25**, 775-786.e775. doi:10.1016/j.chembiol.2018.03.012

Moore, B. S., Stepanchick, A. N., Tewson, P. H., Hartle, C. M., Zhang, J., Quinn, A. M., Hughes, T. E. and Mirshahi, T. (2016). Cilia have high cAMP levels that are inhibited by Sonic Hedgehog-regulated calcium dynamics. *Proc. Natl. Acad. Sci. USA* **113**, 13069-13074. doi:10.1073/pnas.1602393113

Mukhopadhyay, S., Wen, X., Ratti, N., Loktev, A., Rangell, L., Scales, S. J. and Jackson, P. K. (2013). The ciliary G-protein-coupled receptor Gpr161 negatively regulates the Sonic hedgehog pathway via cAMP signaling. *Cell* **152**, 210-223. doi:10.1016/j.cell.2012.12.026

Niewiadomski, P., Kong, J. H., Ahrends, R., Ma, Y., Humke, E. W., Khan, S., Teruel, M. N., Novitch, B. G. and Rohatgi, R. (2014). Gli protein activity is controlled by multisite phosphorylation in vertebrate Hedgehog signaling. *Cell Rep.* **6**, 168-181. doi:10.1016/j.celrep.2013.12.003

Oh, S., Huang, X. and Chiang, C. (2005). Specific requirements of sonic hedgehog signaling during oligodendrocyte development. *Dev. Dyn.* **234**, 489-496. doi:10.1002/dvdy.20422

Ou, Z., Sun, Y., Lin, L., You, N., Liu, X., Li, H., Ma, Y., Cao, L., Han, Y., Liu, M. et al. (2016). Olig2-targeted G-protein-coupled receptor Gpr17 regulates oligodendrocyte survival in response to lysolecithin-induced demyelination. *J. Neurosci.* **36**, 10560-10573. doi:10.1523/JNEUROSCI.0898-16.2016

Pan, Y., Bai, C. B., Joyner, A. L. and Wang, B. (2006). Sonic hedgehog signaling regulates Gli2 transcriptional activity by suppressing its processing and degradation. *Mol. Cell. Biol.* **26**, 3365-3377. doi:10.1128/MCB.26.9.3365-3377.2006

Pan, Y., Wang, C. and Wang, B. (2009). Phosphorylation of Gli2 by protein kinase A is required for Gli2 processing and degradation and the Sonic Hedgehog-regulated mouse development. *Dev. Biol.* **326**, 177-189. doi:10.1016/j.ydbio.2008.11.009

Parravicini, C., Ranghino, G., Abbracchio, M. P. and Fantucci, P. (2008). GPR17: molecular modeling and dynamics studies of the 3-D structure and purinergic ligand binding features in comparison with P2Y receptors. *BMC Bioinformatics* **9**, 263. doi:10.1186/1471-2105-9-263

Parravicini, C., Abbracchio, M. P., Fantucci, P. and Ranghino, G. (2010). Forced unbinding of GPR17 ligands from wild type and R255I mutant receptor models through a computational approach. *BMC Struct. Biol.* **10**, 8. doi:10.1186/1472-6807-10-8

Perrimon, N., Pitsouli, C. and Shilo, B.-Z. (2012). Signaling mechanisms controlling cell fate and embryonic patterning. *Cold Spring Harbor Perspect. Biol.* **4**, a005975. doi:10.1101/cshperspect.a005975

Psychoyos, D. and Finnell, R. (2008). Method for culture of early chick embryos ex vivo (New Culture). *J. Vis. Exp.* **20**, 193-197. doi:10.3791/903

Pusapati, G. V., Kong, J. H., Patel, B. B., Gouti, M., Sagner, A., Sircar, R., Luchetti, G., Ingham, P. W., Briscoe, J. and Rohatgi, R. (2018). G protein-coupled receptors control the sensitivity of cells to the morphogen Sonic Hedgehog. *Sci. Signal.* **11**, eaao5749. doi:10.1126/scisignal.aao5749

Rehimi, R., Nikolic, M., Cruz-Molina, S., Tebartz, C., Frommolt, P., Mahabir, E., Clément-Ziza, M. and Rada-Iglesias, A. (2016). Epigenomics-based identification of major cell identity regulators within heterogeneous cell populations. *Cell Rep.* **17**, 3062-3076. doi:10.1016/j.celrep.2016.11.046

Ribes, V. and Briscoe, J. (2009). Establishing and interpreting graded Sonic Hedgehog signaling during vertebrate neural tube patterning: the role of negative feedback. *Cold Spring Harbor Perspect. Biol.* **1**, a002014. doi:10.1101/cshperspect.a002014

Rosenbaum, D. M., Rasmussen, S. G. F. and Kobilka, B. K. (2009). The structure and function of G-protein-coupled receptors. *Nature* **459**, 356-363. doi:10.1038/nature08144

Sasai, N. and Briscoe, J. (2012). Primary cilia and graded Sonic Hedgehog signaling. *Wiley Interdiscip. Rev. Dev. Biol.* **1**, 753-772. doi:10.1002/wdev.43

Sasai, N., Kutejova, E. and Briscoe, J. (2014). Integration of signals along orthogonal axes of the vertebrate neural tube controls progenitor competence and increases cell diversity. *PLoS Biol.* **12**, e1001907. doi:10.1371/journal.pbio.1001907

Sasaki, H., Nishizaki, Y., Hui, C., Nakafuku, M. and Kondoh, H. (1999). Regulation of Gli2 and Gli3 activities by an amino-terminal repression domain: implication of Gli2 and Gli3 as primary mediators of Shh signaling. *Development* **126**, 3915-3924.

Simon, K., Hennen, S., Merten, N., Blättermann, S., Gillard, M., Kostenis, E. and Gomeza, J. (2016). The Orphan G protein-coupled receptor GPR17 negatively regulates oligodendrocyte differentiation via Galphai/o and Its downstream effector molecules. *J. Biol. Chem.* **291**, 705-718. doi:10.1074/jbc.M115.683953

Singh, J., Wen, X. and Scales, S. J. (2015). The Orphan G protein-coupled receptor Gpr175 (Tpra40) enhances hedgehog signaling by modulating cAMP levels. *J. Biol. Chem.* **290**, 29663-29675. doi:10.1074/jbc.M115.665810

Stamataki, D., Ulloa, F., Tsoni, S. V., Mynett, A. and Briscoe, J. (2005). A gradient of Gli activity mediates graded Sonic Hedgehog signaling in the neural tube. *Genes Dev.* **19**, 626-641. doi:10.1101/gad.325905

Tempe, D., Casas, M., Karaz, S., Blanchet-Tournier, M.-F. and Concordet, J.-P. (2006). Multisite protein kinase A and glycogen synthase kinase 3beta phosphorylation leads to Gli3 ubiquitination by SCFbetaTrCP. *Mol. Cell. Biol.* **26**, 4316-4326. doi:10.1128/MCB.02183-05

Tuson, M., He, M. and Anderson, K. V. (2011). Protein kinase A acts at the basal body of the primary cilium to prevent Gli2 activation and ventralization of the mouse neural tube. *Development* **138**, 4921-4930. doi:10.1242/dev.070805

Vuolo, L., Herrera, A., Torroba, B., Menendez, A. and Pons, S. (2015). Ciliary adenylyl cyclases control the Hedgehog pathway. *J. Cell Sci.* **128**, 2928-2937. doi:10.1242/jcs.172635

Wang, B. and Li, Y. (2006). Evidence for the direct involvement of {beta}TrCP in Gli3 protein processing. *Proc. Natl. Acad. Sci. USA* **103**, 33-38. doi:10.1073/pnas.0509927103

Wang, B., Fallon, J. F. and Beachy, P. A. (2000). Hedgehog-regulated processing of Gli3 produces an anterior/posterior repressor gradient in the

developing vertebrate limb. *Cell* **100**, 423-434. doi:10.1016/S0092-8674(00)80678-9

Wang, S.-Z., Dulin, J., Wu, H., Hurlock, E., Lee, S.-E., Jansson, K. and Lu, Q. R. (2006). An oligodendrocyte-specific zinc-finger transcription regulator cooperates with Olig2 to promote oligodendrocyte differentiation. *Development* **133**, 3389-3398. doi:10.1242/dev.02522

Wolpert, L. (1969). Positional information and the spatial pattern of cellular differentiation. *J. Theor. Biol.* **25**, 1-47. doi:10.1016/S0022-5193(69)80016-0

Ying, Q.-L., Stavridis, M., Griffiths, D., Li, M. and Smith, A. (2003). Conversion of embryonic stem cells into neuroectodermal precursors in adherent monoculture. *Nat. Biotechnol.* **21**, 183-186. doi:10.1038/nbt780

Zhou, Q. and Anderson, D. J. (2002). The bHLH transcription factors OLIG2 and OLIG1 couple neuronal and glial subtype specification. *Cell* **109**, 61-73. doi:10.1016/S0092-8674(02)00677-3

Zhou, Q., Choi, G. and Anderson, D. J. (2001). The bHLH transcription factor Olig2 promotes oligodendrocyte differentiation in collaboration with Nkx2.2. *Neuron* **31**, 791-807. doi:10.1016/S0896-6273(01)00414-7